

# Reentrant Superspin Glass Phase in a $\text{La}_{0.82}\text{Ca}_{0.18}\text{MnO}_3$ Ferromagnetic Insulator

P. Anil Kumar,<sup>1,2</sup> R. Mathieu,<sup>2</sup> P. Nordblad,<sup>2</sup> Sugata Ray,<sup>1,3</sup> Olof Karis,<sup>4</sup> Gabriella Andersson,<sup>4</sup> and D. D. Sarma<sup>1,4,5,\*</sup>

<sup>1</sup>*Centre for Advanced Materials, Indian Association for the Cultivation of Science, Kolkata 700032, India*

<sup>2</sup>*Department of Engineering Sciences, Uppsala University, P.O. Box 534, SE-751 21 Uppsala, Sweden*

<sup>3</sup>*Department of Materials Science, Indian Association for the Cultivation of Science, Kolkata 700032, India*

<sup>4</sup>*Department of Physics and Astronomy, Uppsala University, Box-516, 75120 Uppsala, Sweden*

<sup>5</sup>*Solid State and Structural Chemistry Unit, Indian Institute of Science, Bangalore 560012, India*

(Received 25 September 2013; revised manuscript received 27 November 2013; published 12 March 2014)

We report results of the magnetization and ac susceptibility measurements down to very low fields on a single crystal of the perovskite manganite,  $\text{La}_{0.82}\text{Ca}_{0.18}\text{MnO}_3$ . This composition falls in the intriguing ferromagnetic insulator region of the manganite phase diagram. In contrast to earlier beliefs, our investigations reveal that magnetically (and in every other sense), this is a single-phase system with a ferromagnetic ordering temperature of around 170 K. However, this ferromagnetic state is magnetically frustrated, and the system exhibits pronounced glassy dynamics below 90 K. Based on measured dynamical properties, we propose that this quasi-long-ranged ferromagnetic phase, and the associated superspin glass behavior, is the true magnetic state of the system, rather than being a macroscopic mixture of ferromagnetic and antiferromagnetic phases, as often suggested. Our results provide an understanding of the quantum phase transition from an antiferromagnetic insulator to a ferromagnetic metal via this ferromagnetic insulating state as a function of  $x$  in  $\text{La}_{1-x}\text{Ca}_x\text{MnO}_3$ , in terms of the possible formation of magnetic polarons.

## I. INTRODUCTION

Hole-doped perovskite manganites of the general formula  $A_{1-x}B_x\text{MnO}_3$  ( $A$  = trivalent lanthanide;  $B$  = divalent alkali metal) with a low doping, generally  $0.05 < x < 0.22$  for  $A = \text{La}$  and  $B = \text{Ca}$ , are of fundamental interest because they constitute the few examples of ferromagnetic insulators, unlike the ones with higher  $x$  or a larger bandwidth, which are ferromagnetic but also metallic, or with a lower  $x$ , which are insulating but also antiferromagnetic [1]. While the origin of a ferromagnetic, insulating state in some undoped compounds, such as  $\text{La}_2\text{NiMnO}_6$  [2,3], has been explained in the past, charge doped systems present additional difficulties in comprehending a ferromagnetic insulating ground state. Specifically, the origin of the coexistence of ferromagnetic and insulating properties in  $\text{La}_{1-x}\text{Ca}_x\text{MnO}_3$  (LCMO) has not been established. The ferromagnetic metallic (FMM) phase of the perovskite manganites with larger doping has been successfully explained by the double exchange mechanism proposed by Zener [4,5]. This mechanism, while

explaining the ferromagnetism, invariably requires the system to be metallic because of the hopping of electrons between  $\text{Mn}^{3+}$  and  $\text{Mn}^{4+}$ , hence failing to explain the ferromagnetic insulating state. Furthermore, we note that electronic phase separation of varying length scales has been reported at higher Ca doping levels [6].

A major obstacle in establishing the true ground state in the case of manganites has been the difficulty in preparing single phase samples, which has led to the speculation [7,8] that the ferromagnetic insulating (FMI) state is the result of spatially distinct coexistence of separate ferromagnetic metallic and antiferromagnetic insulating phases in a single sample. However, investigations performed using other single crystal samples have suggested microscopically homogeneous electronic properties of the samples [9–11]. Interestingly, even the reports on these homogeneous samples are interpreted in order to promote contrasting pictures for the magnetic ground state. For example, the authors of Refs. [9,10] observed a non-diverging magnetic correlation length and signatures of short-range magnetic polarons using neutron-scattering experiments, while a much more recent work [11] suggested an ideal three-dimensional Heisenberg ferromagnetic ground state, based on the values of the critical exponents that they obtain for the FMI composition of LCMO. Nevertheless, both theory and experiments suggest the formation of local lattice distortions or lattice polarons in the ordered state leading to a nanoscale inhomogeneity that is starkly different from the chemical or macroscopic electronic phase separation [10,12–16].

\*Also at Jawaharlal Nehru Centre for Advanced Scientific Research, Bangalore and Council of Scientific and Industrial Research-Network of Institutes for Solar Energy (CSIR-NISE). sarma@sscu.iisc.ernet.in

Published by the American Physical Society under the terms of the Creative Commons Attribution 3.0 License. Further distribution of this work must maintain attribution to the author(s) and the published article's title, journal citation, and DOI.

The ac susceptibility technique can be useful in determining the true magnetic state of a material. An enlightening report on the magnetic properties of a single crystal of  $\text{La}_{0.8}\text{Ca}_{0.2}\text{MnO}_3$ , which is closer to the FMM composition, using ac techniques is found in Ref. [17], however without considering nonequilibrium (aging) and nonlinear field effects. Here, we investigate in detail the static and dynamical magnetic properties of a single crystal of  $\text{La}_{0.82}\text{Ca}_{0.18}\text{MnO}_3$  (LCMO18) whose composition lies within the FMI regime ( $0.05 < x < 0.22$ ). It is found that the material orders ferromagnetically, albeit displaying glassy dynamics. The observed glassy dynamics suggest that frustration effects govern the ferromagnetic configuration, as in reentrant spin-glass systems (reentrant ferromagnet in the present case). However, the significant difference is that the magnetic entities in the present case are groups of spins (magnetic polarons), instead of the single spins of conventional reentrant magnets or spin glasses, i.e., a reentrant superspin glass state. The results indicate that the reentrant ferromagnetic insulating state is the intrinsic magnetic state of this composition, rather than a (macroscopically) phase separated one. We discuss the microscopic nature and origin of the ferromagnetic insulating phase, as well as the transition to ferromagnetic metal for larger hole doping.

## II. EXPERIMENTAL DETAILS

$\text{La}_{0.82}\text{Ca}_{0.18}\text{MnO}_3$  single crystal pieces are grown by a floating zone technique (Crystal Systems Corporation, Japan) starting from a single phase polycrystalline sample of the same composition. To compensate for the Mn evaporation during crystal growth, an additional 1% MnO is added. The phase purity of the final grown crystal is verified by powder x-ray diffraction (XRD) using a Bruker D8 Advance diffractometer. Spot analysis of energy dispersive x-ray spectroscopy on a JEOL FESEM reveals that the cation distribution in the plane perpendicular to the growth direction is uniform and that the cation concentrations are also close to the nominal composition. The correct stoichiometry of the single crystals is additionally verified by inductively coupled plasma-optical emission spectroscopy (ICP-OES) using a Perkin Elmer instrument. The electronic transport measurements are carried out using a laboratory setup and PPMS from Quantum Design Inc. PPMS is also used for heat capacity measurements. Magnetization  $M$  and ac susceptibility (in-phase component  $\chi'$  and out-of-phase component  $\chi''$ ) data are collected, on a roughly rectangular piece of 5-mm  $\times$  1.2-mm  $\times$  1.5-mm crystal, using the Quantum Design MPMS XL SQUID magnetometer. Magneto-optic Kerr effect (MOKE) images are recorded at temperatures between 80 K and 273 K using a polarizing microscope with an external field applied in the plane of the sample and parallel to the scattering plane of the light (longitudinal MOKE configuration).

## III. RESULTS AND DISCUSSION

In Fig. 1(a), we present the temperature dependence of the electrical resistance  $R$  of the LCMO18 single crystal. A weak signature of the insulator-to-metal transition can be observed in the zero-magnetic-field data at about 170 K before reentering an insulating state on further lowering the temperature below about 140 K. It is in agreement with the earlier literature data [18] for this composition; this fact also ensures the quality of the sample since the electronic transport behavior is most sensitive to the oxygen non-stoichiometry and compositional variation. The associated magnetoresistance (MR) observed in 40 kOe applied field is also indicated in the figure. Interestingly, this composition also exhibits colossal electroresistance (CER) [19,20], as demonstrated in Fig. 1(b) and the inset. The resistance of the crystal is indeed highly sensitive to the magnitude of the current that passes through the sample. The inset shows the reversible switching of sample resistance with applied voltage. Corresponding results on MR and CER of LCMO have been reported in the literature; however, the details of the large electroresistance are different [19,20].

In Fig. 2(a), we show the zero-field-cooled (ZFC) and field-cooled (FC) magnetization as a function of temperature. In the ZFC curve, a sharp rise in  $M$  resembling a magnetic transition is observed near 170 K, coinciding with the insulator-metal transition temperature [cf. Fig. 1(a)]. In

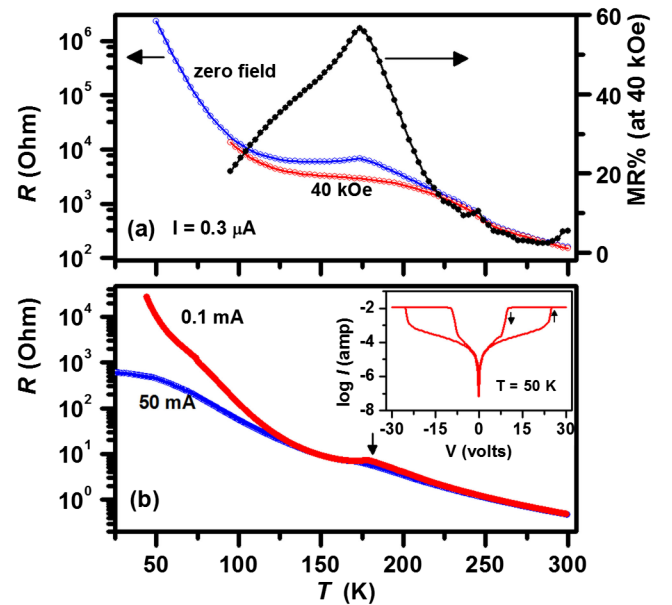


FIG. 1 (a) Temperature dependence of the electrical resistance  $R$  of LCMO18 recorded under zero and 40 kOe field. The third curve (right axis) shows the associated magnetoresistance  $\text{MR}\% = 100 \times (R(H=0) - R(H=40 \text{ kOe})) / R(H=0)$ . (b) The behavior of  $R$  with temperature  $T$  for different excitation currents to exemplify the electroresistance behavior. The inset in panel (b) shows a typical  $I$ - $V$  curve recorded at  $T = 50 \text{ K}$ . The flat region in the curve is due to the current limit, 10 mA, of the electrometer.

addition, a drop in ZFC magnetization is observed around 70 K on lowering the temperature. This second anomaly is not reflected in the heat capacity ( $C$ ) curve depicted in the inset of Fig. 2(a). However, a peak is observed in the heat capacity curve in the vicinity of the first magnetic transition, confirming the enhanced magnetic correlations in the system. The peak in heat capacity is relatively broad, suggesting that the long-range ordering of the ferromagnetic state established below 170 K is hindered [21]. Interestingly, the magnetization-field (hysteresis) loops measured at different temperatures across the two anomalies in the  $M(T)$  curve, presented in Fig. 2(b), show ferromagnetic behavior at and below 150 K, in line with the magnetic ordering at 170 K. The saturation moment per Mn (about  $3.78 \mu_B$ ) at 10 K is very close to the value ( $3.82 \mu_B$ ) expected for a full ferromagnetic arrangement of Mn ions in the system. The temperature and magnetic field dependence of the magnetization hence suggests that the system is ferromagnetically ordered below 170 K, however with hindered critical divergence at  $T_C$ . Yet, the high field magnetic moment (for fields larger than 10 kOe) corresponds to full polarization of that ferromagnetic state, suggesting the lack of macroscopic phase separation into ferromagnetic and antiferromagnetic regions. Furthermore, Kerr microscopy images collected on our crystal at 100 K

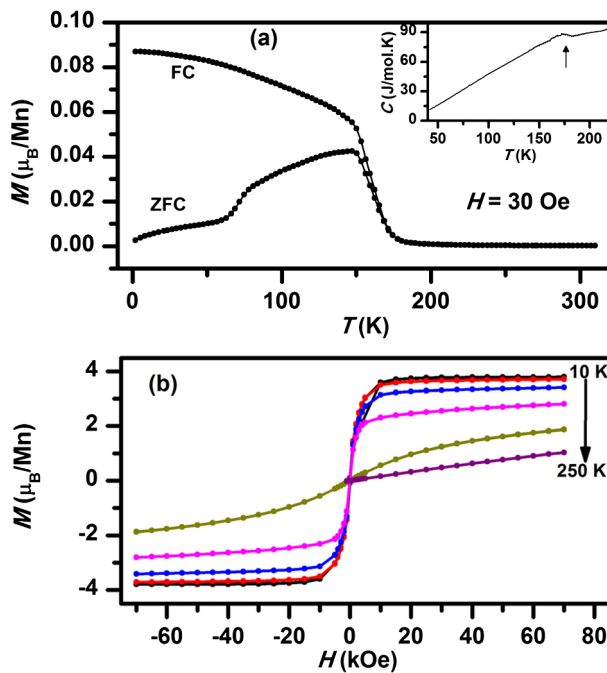


FIG. 2 (a) Temperature dependence of the zero-field-cooled (ZFC) and field-cooled (FC) magnetization in a 30 Oe field. The inset shows the temperature dependence of the heat capacity  $C$  measured upon heating. (b) Magnetic field dependence of the magnetization (hysteresis loops) measured at different temperatures (10, 50, 100, 150, 200, and 250 K). Only positive field data is presented for 250 K at which the sample is paramagnetic.

did not show any domain structure within the instrumental resolution limit of  $0.5 \mu\text{m}$ . However, the magneto-optic Kerr effect (MOKE) intensity follows the bulk magnetization value, as shown in Fig. 3. The MOKE data correspond to a  $425 \times 325 \mu\text{m}^2$  area of the crystal with the field applied in the same plane as for the bulk magnetization measurement.

The result of temperature dependent ac susceptibility measurements is presented in Fig. 4. Data collected using three different ac-field amplitudes,  $h$ , are shown. As seen in the figure, the temperature dependence of the in- and out-of-phase components of the susceptibility is qualitatively similar for all amplitudes of the ac probing field. For example, the  $\chi'(T)$  curves include a sharp peak near 170 K and a drop in the susceptibility below 90 K, akin to the features observed in the ZFC magnetization presented in Fig. 2(a). Sharp peaks near 170 K and drops below 90 K are also observed for all amplitudes in  $\chi''(T)$  curves. The low field susceptibility is strongly nonlinear and enhanced by the amplitude of the ac field,  $h$  (see, e.g., the 100–150 K temperature interval for different values of  $h$ ). Additional measurements as a function of amplitude  $h$  show that the response of the system is essentially linear, at least up to 0.5 Oe at temperatures below 140 K. Hence, we choose an amplitude of 0.4 Oe for all subsequent ac magnetic measurements in order to study the intrinsic magnetism of the material. For this amplitude, the ac-susceptibility curves (see left panels of Fig. 5) are reminiscent of those of reentrant ferromagnets, which exhibit two peaks in the  $\chi'(T)$  curves reflecting ferromagnetic and spin-glass phase transitions, respectively [3,22,23]; the higher temperature transition shows no frequency dispersion, while the low temperature transition shows clear frequency dispersion. Spin glass states result from frustration effects due to the presence of competing magnetic interactions (the frustration may also be geometric). Furthermore, particulates of ferromagnetic domains may also exhibit glassy magnetic features when the particulate size is low enough [24]. It is also important to note that the spin correlation length does not diverge at the ferromagnetic transition temperature in the FMI composition of LCMO, suggesting the formation

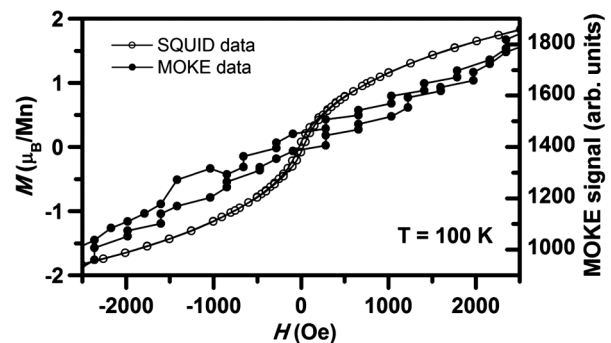


FIG. 3 Comparison of MOKE intensity to the bulk magnetization curve (SQUID data) measured at 100 K.

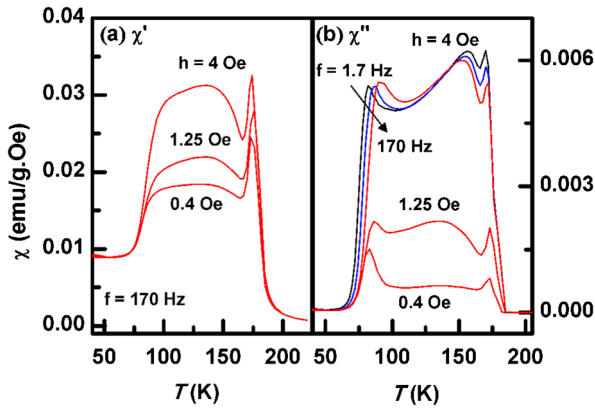


FIG. 4 Temperature dependence of the (a) in-phase  $\chi'$  and (b) out-of-phase  $\chi''$  components of the ac susceptibility recorded using different amplitudes of the probing ac field ( $h = 0.4, 1.25,$  and  $4$  Oe). The frequency  $f$  is  $170$  Hz.  $\chi''$  (T) data obtained for  $1.7$  and  $17$  Hz are also plotted for  $h = 4$  Oe as an indication of dynamical behavior.

of nanoscopic ferromagnetic domains at the transition temperature [9].

In the susceptibility curves presented in the left panels [(a) and (b)] of Fig. 5, the onset of the high temperature peak is frequency independent, as expected for a ferromagnetic transition, while the lower temperature peak is quite frequency dependent, suggesting a low-temperature glassy behavior. It is remarkable that, as observed in systems with blocked magnetic clusters, the magnitude of  $\chi''(T)$  drops very rapidly below the low-temperature peak and remains at or near zero, with negligible frequency dependence, on further lowering of the temperature. This behavior suggests that the fundamental entities of this glassy transition are groups of coherent spins (superspins) rather than individual atomic spins [22,25].

The low temperature ac susceptibility of spin glasses is weakly affected by low superimposed dc magnetic fields. This is also the case in LCMO18, as seen in the right panels [(c) and (d)] of Fig. 5. A magnetic field of  $50$  Oe slightly affects the susceptibility curve in the whole measured range of temperatures. However, a field of  $500$  Oe significantly reduces the ac susceptibility above  $80$  K. The ac susceptibility of the low temperature phase is essentially unaffected by the superimposed magnetic field, akin to reentrant ferromagnets [22].

Although disordered, spin glass materials undergo a magnetic phase transition at a temperature  $T_g$  with well-established critical exponents. If a spin glass is cooled down below  $T_g$ , it will always be out of equilibrium, and its spin configuration will rearrange itself toward the equilibrium configuration for that temperature [26,27]. This equilibration is referred to as aging [27–29]. Aging can be observed in relaxation experiments, in which a dc or ac excitation is used to record the isothermal magnetization or susceptibility as a function of time [27,30]. If the temperature is changed, the system will again rearrange itself toward the equilibrium configuration of the new temperature; the system will be reinitialized or rejuvenated. Yet, it can be shown that the spin configuration resulting from the first equilibration is kept in memory even though the second equilibration takes place [27,31]. If the new temperature is lower than the initial one, the system equilibrates to a configuration corresponding to the new temperature and keeps the equilibrated configuration of the higher temperature in memory. On the other hand, if the new temperature is higher than the initial one, the system will be reinitialized, even for short durations at the new temperature.

Some systems will first order magnetically as long-ranged ferromagnets or antiferromagnets to become (or reenter) a disordered phase at low temperatures. This is the

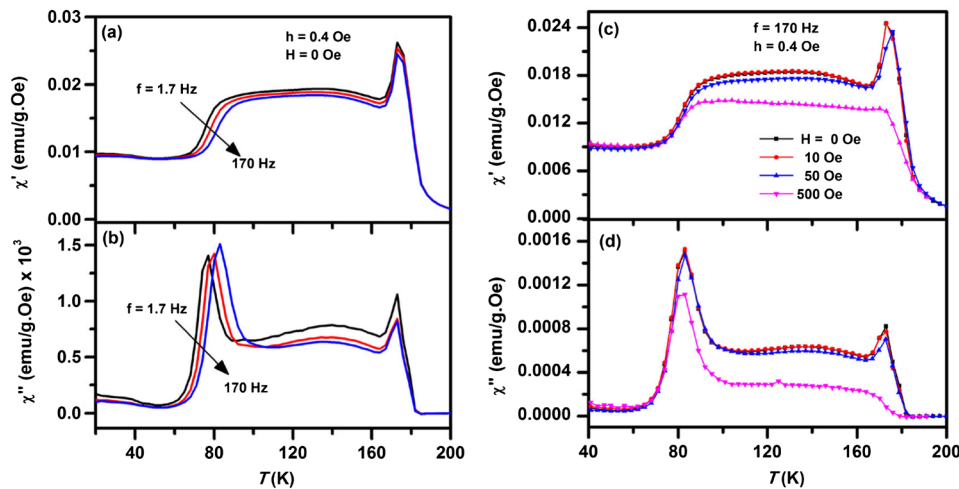


FIG. 5 Temperature dependence of the (upper panels) in-phase  $\chi'$  and (lower panels) out-of-phase  $\chi''$  components of the ac susceptibility recorded for (a, b) different frequencies ( $f = 1.7, 17,$  and  $170$  Hz;  $h = 0.4$  Oe) and (c, d) under different superimposed dc magnetic fields ( $H = 0, 10, 50,$  and  $500$  Oe;  $f = 170$  Hz;  $h = 0.4$  Oe).

case of reentrant spin glasses or, in the case of ferromagnets, reentrant ferromagnets [23]. The disordered phase is a consequence of the magnetic frustration in the ordered phase, hindering the perfect ordering. It has been shown that the low-temperature spin glass phase of such materials has a similar dynamical behavior as those of ordinary spin glasses, and also that the ferromagnetic phase exhibits glassy features and aging, although the spin configuration of this phase reinitializes upon both positive and negative temperature cycling, unlike in spin glasses [32]. While the critical slowing down at the spin glass phase transition can be investigated by, e.g., scaling analyses of the onset of  $\chi''$  in ac-susceptibility measurements [26], such analyses are difficult in reentrant ferromagnets because of the “parasitic” ferromagnetic phase contributing to the susceptibility [22,23]. Nevertheless, the onset of a low temperature glassy phase is indicated by the frequency dependence of the low-temperature peak of the  $\chi$ - $T$  curves.

Aging phenomena are observed in LCMO18 at temperatures below 170 K. As illustrated in Fig. 6(a),  $\chi''$  relaxes downwards at constant temperature after being cooled from a reference temperature in the paramagnetic region ( $T_{\text{ref}} = 220$  K). Yet, the shape and magnitude of the relaxation of the  $\chi'(t)$  curves are quite different at temperatures above and below the low temperature peak. The inset in Fig. 6(a) shows the relaxation at 60 K in an expanded scale to clearly illustrate the difference in shape of the relaxation in the ferromagnetic and glassy phases of the sample. The time-dependent susceptibility data recorded at various temperatures from 50 to 180 K are plotted (vertical lines) in Figs. 6(b) and 6(c) as a function of temperature. For comparison, a conventional temperature-dependent ac susceptibility data recorded using the same frequency and excitation ( $f = 1.7$  Hz,  $h = 0.4$  Oe) is also plotted. We can see in those panels that the weak downward relaxation observed at 50, 60, and 70 K starts from about the same susceptibility values as those obtained in the ordinary temperature-dependent measurement. This is similar to what is expected and observed in spin glass states [27,30]. For temperatures above 70 K, the behavior is quite different, and one can see [more clearly in Fig. 6(c)] that the relaxation starts from higher values of the ac susceptibility and finishes below the T-dependent values on the longest time observed in our experiments (3600 s). This behavior is reminiscent of that of the ferromagnetic phase of a reentrant ferromagnet [32]. The difference in relaxation behavior between the two temperature regions (above and below 80 K) is again evidence of the phase change from a frustrated ferromagnetically dominated response to a glassy one.

Coming back to the origin of the magnetic behavior in these compounds, there are some plausible explanations [16,33,34], such as the two-electron fluid  $lb$  model; one type of electrons are essentially localized, combined with a distortion of  $\text{MnO}_6$  octahedra (polaronic), while the other

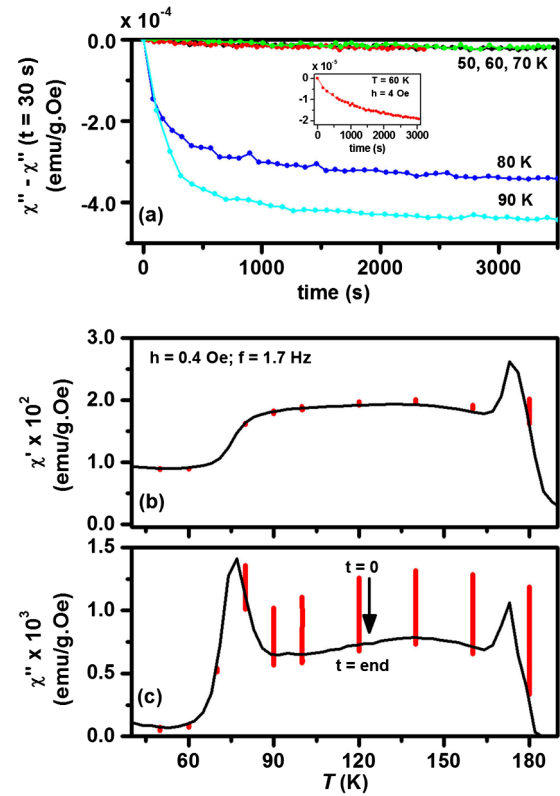


FIG. 6 (a): Time dependence of the normalized out-of-phase susceptibility for different temperatures recorded, after a quench from 220 K, at  $T = 50, 60, 70, 80,$  and  $90$  K. The inset shows a similar curve measured at 60 K but using a higher field amplitude,  $h = 4$  Oe. (b) and (c): The time-dependent data presented in the upper panel are plotted as a function of temperature, for the in-phase and out-of phase components of the susceptibility, without normalization. The top of the vertical lines corresponds to a susceptibility value at  $t = 0$  s, and the bottom corresponds to the end time (3600 s). Additional data obtained for  $T = 100, 120, 140, 160,$  and  $180$  K are included. The results of an ordinary temperature dependent measurement of the ac susceptibility are included [ $\chi'(T)$  and  $\chi''(T)$  curves, respectively] ( $f = 170$  Hz;  $h = 0.4$  Oe).

type are characterized by finite hopping and a nondistorted lattice. One of the experimental proofs for such a scenario comes from the extended x-ray absorption fine-structure (EXAFS) analysis [35–37]. The microscopic crystal structure is probed using EXAFS in several doped manganite samples or crystals, focusing on the fraction of Jahn-Teller (JT) distorted  $\text{MnO}_6$  octahedra in the lattice.  $\text{Mn}^{3+}$  is JT active while the  $\text{Mn}^{4+}$  is JT inactive; in doped manganites, there is a mixture of both. It was concluded that in the FMM samples, the JT distortion is completely removed in the fully magnetized state of the sample, which is achieved either by lowering the temperature or by application of an external magnetic field. However, in the case of FMI samples, there exists JT-distorted  $\text{MnO}_6$  octahedra even in the ferromagnetic state; nevertheless, the application of a relatively large magnetic field leads to a reduction in the

fraction of JT-distorted  $\text{MnO}_6$  octahedra [36]. These observations are linked to the fact that in FMM samples, the  $e_g$  electrons are completely itinerant, and hence, no Mn ions are JT active; in contrast, in the FMI samples, the  $e_g$  electrons are localized between neighboring Mn ions, and hence, some Mn ions are JT active. Because of such a combination of polaronic and nonpolaronic  $\text{MnO}_6$  octahedra in the FMI compositions, the magnetic properties are also expected to be different from the ferromagnetic ground states that are observed in metallic compositions. The solid-state nuclear magnetic resonance (NMR) experiments on LCMO samples have also pointed to the presence of different fractions of FMI and FMM phases depending on the composition and temperature [38]. Our results suggest that the magnetic and electrical properties with hole doping in low-bandwidth manganites evolve from an antiferromagnetic insulator (AFI) at the lowest doping levels via a frustrated ferromagnetic insulator for intermediate doping to the FMM at higher doping.

#### IV. CONCLUSIONS

We have reported the results of dc and ac magnetic characterization of a single crystal of  $\text{La}_{0.82}\text{Ca}_{0.18}\text{MnO}_3$ , which belongs to the fundamentally interesting composition range of a ferromagnetic insulating phase in the family of manganites. The dc and ac magnetic measurements combined suggest that the low temperature magnetic state of this composition is a reentrant ferromagnet. In other words, LCMO18 enters a frustrated ferromagnetic state at 170 K followed by a reentrant superspin glass state at about 80 K that is transformed to a fully magnetized ferromagnetic state by a large enough magnetic field. This intrinsic glassy magnetic state is in accordance with the results of theoretical models and EXAFS experiments on the low doped manganites, which predict magnetic polaron formation. A correlated group of such polarons that make up the superspins can be termed nanoscopic phase separation.

#### ACKNOWLEDGMENTS

The authors thank the Department of Science and Technology, as well as Council of Scientific and Industrial Research, Government of India and the Swedish Foundation for International Cooperation in Research and Higher Education (STINT) for supporting this research. P. A. K., R. M., and P. N. thank the Swedish Research Council (VR) and the Göran Gustafsson Foundation, Sweden for funding.

- 
- [1] E. Dagotto, T. Hotta, and A. Moreo, *Colossal Magnetoresistant Materials: The Key Role of Phase Separation*, *Phys. Rep.* **344**, 1 (2001).  
 [2] H. Das, U. V. Waghmare, T. Saha-Dasgupta, and D. D. Sarma, *Electronic Structure, Phonons, and Dielectric*

- Anomaly in Ferromagnetic Insulating Double Pervoskite  $\text{La}_2\text{NiMnO}_6$* , *Phys. Rev. Lett.* **100**, 186402 (2008).  
 [3] D. Choudhury, P. Mandal, R. Mathieu, A. Hazarika, S. Rajan, A. Sundaresan, U. V. Waghmare, R. Knut, O. Karis, P. Nordblad, and D. D. Sarma, *Near-Room-Temperature Colossal Magnetodielectricity and Multiglass Properties in Partially Disordered  $\text{La}_2\text{NiMnO}_6$* , *Phys. Rev. Lett.* **108**, 127201 (2012).  
 [4] C. Zener, *Interaction between the d-Shells in the Transition Metals. II. Ferromagnetic Compounds of Manganese with Pervoskite Structure*, *Phys. Rev.* **82**, 403 (1951).  
 [5] P. G. de Gennes, *Effects of Double Exchange in Magnetic Crystals*, *Phys. Rev.* **118**, 141 (1960).  
 [6] V. B. Shenoy, D. D. Sarma, and C. N. R. Rao, *Electronic Phase Separation in Correlated Oxides: The Phenomenon, Its Present Status and Future Prospects*, *ChemPhysChem* **7**, 2053 (2006).  
 [7] V. Markovich, E. Rozenberg, A. I. Shames, G. Gorodetsky, I. Fita, K. Suzuki, R. Puzniak, D. A. Shulyatev, and Y. M. Mukovskii, *Magnetic, Transport, and Electron Magnetic Resonance Properties of  $\text{La}_{0.82}\text{Ca}_{0.18}\text{MnO}_3$  Single Crystals*, *Phys. Rev. B* **65**, 144402 (2002).  
 [8] V. Markovich, I. Fita, R. Puzniak, M. I. Tsindlekht, A. Wisniewski, and G. Gorodetsky, *Magnetization and AC Susceptibility Studies of the Magnetic Phase Separation in  $\text{La}_{0.8}\text{Ca}_{0.2}\text{MnO}_3$  and  $\text{La}_{0.78}\text{Ca}_{0.22}\text{MnO}_3$  Single Crystals*, *Phys. Rev. B* **66**, 094409 (2002).  
 [9] P. C. Dai, J. A. Fernandez-Baca, E. W. Plummer, Y. Tomioka, and Y. Tokura, *Magnetic Coupling in the Insulating and Metallic Ferromagnetic  $\text{La}_{1-x}\text{Ca}_x\text{MnO}_3$* , *Phys. Rev. B* **64**, 224429 (2001).  
 [10] P. C. Dai, J. A. Fernandez-Baca, N. Wakabayashi, E. W. Plummer, Y. Tomioka, and Y. Tokura, *Short-Range Polaron Correlations in the Ferromagnetic  $\text{La}_{1-x}\text{Ca}_x\text{MnO}_3$* , *Phys. Rev. Lett.* **85**, 2553 (2000).  
 [11] W. Jiang, X. Z. Zhou, G. Williams, R. Privezentsev, and Y. Mukovskii, *Mechanisms underlying Ferromagnetism across the Metal-Insulator Transition in  $\text{La}_{1-x}\text{Ca}_x\text{MnO}_3$* , *Phys. Rev. B* **79**, 214433 (2009).  
 [12] R. Mathieu, D. Akahoshi, A. Asamitsu, Y. Tomioka, and Y. Tokura, *Colossal Magnetoresistance without Phase Separation: Disorder-Induced Spin Glass State and Nanometer Scale Orbital-Charge Correlation in Half Doped Manganites*, *Phys. Rev. Lett.* **93**, 227202 (2004).  
 [13] D. D. Sarma, D. Topwal, U. Manju, S. R. Krishnakumar, M. Bertolo, S. La Rosa, G. Cautero, T. Y. Koo, P. A. Sharma, S.-W. Cheong, and A. Fujimori, *Direct Observation of Large Electronic Domains with Memory Effect in Doped Manganites*, *Phys. Rev. Lett.* **93**, 097202 (2004).  
 [14] R. Mathieu, and Y. Tokura, *The Nanoscale Phase Separation in Hole-Doped Manganites*, *J. Phys. Soc. Jpn.* **76**, 124706 (2007).  
 [15] S. Cengiz, G. Alvarez, and E. Dagotto, *Competing Ferromagnetic and Charge-Ordered States in Models for Manganites: The Origin of the Colossal Magnetoresistance Effect*, *Phys. Rev. Lett.* **98**, 127202 (2007).  
 [16] V. B. Shenoy, Tribikram Gupta, H. R. Krishnamurthy, and T. V. Ramakrishnan, *Coulomb Interactions and Nanoscale Electronic Inhomogeneities in Manganites*, *Phys. Rev. Lett.* **98**, 097201 (2007).

- [17] C. P. Hong, E. O. Chi, W. S. Kim, N. H. Hur, and Y. N. Choi, *Magnetic Glassiness below Curie Temperature in  $\text{La}_{0.8}\text{Ca}_{0.2}\text{MnO}_3$* , *J. Phys. Soc. Jpn.* **71**, 1583 (2002).
- [18] X. D. Wu, K. Suzuki, J. Cochrane, V. Markovich, and G. Gorodetsky, *Effect of Electrical Current on Magnetic and Transport Properties of Single-Crystalline  $\text{La}_{0.82}\text{Ca}_{0.18}\text{MnO}_3$* , *IEEE Trans. Magn.* **46**, 1705 (2010).
- [19] Y. Yuzhelevski, V. Markovich, V. Dikovskiy, E. Rozenberg, G. Gorodetsky, G. Jung, D. A. Shulyatev, and Y. M. Mukovskii, *Current-Induced Metastable Resistive States with Memory in Low-Doped Manganites*, *Phys. Rev. B* **64**, 224428 (2001).
- [20] H. Jain, A. K. Raychaudhuri, Y. M. Mukovskii, and D. Shulyatev, *Colossal Electroresistance and Current Induced Switching in Ferromagnetic Insulating State of  $\text{La}_{0.82}\text{Ca}_{0.18}\text{MnO}_3$* , *Appl. Phys. Lett.* **89**, 152116 (2006).
- [21] M. Egilmez, K. H. Chow, J. Jung, I. Fan, A. I. Mansour, and Z. Salman, *Metal-Insulator Transition, Specific Heat, and Grain-Boundary-Induced Disorder in  $\text{Sm}_{0.55}\text{Sr}_{0.45}\text{MnO}_3$* , *Appl. Phys. Lett.* **92**, 132505 (2008).
- [22] K. Jonason, J. Mattsson, and P. Nordblad, *Dynamic Susceptibility of a Reentrant Ferromagnet*, *Phys. Rev. B* **53**, 6507 (1996).
- [23] R. Mathieu, P. Svedlindh, and P. Nordblad, *Re-entrant Spin Glass Transition in  $\text{La}_{0.96-y}\text{Nd}_y\text{K}_{0.04}\text{MnO}_3$ : Origin and Effects on the Colossal Magnetoresistivity*, *Europhys. Lett.* **52**, 441 (2000).
- [24] J. Wu and C. Leighton, *Glassy Ferromagnetism and Magnetic Phase Separation in  $\text{La}_{1-x}\text{Sr}_x\text{CoO}_3$* , *Phys. Rev. B* **67**, 174408 (2003).
- [25] M. F. Hansen, P. E. Jönsson, P. Nordblad, and P. Svedlindh, *Critical Dynamics of an Interacting Magnetic Nanoparticle System*, *J. Phys. Condens. Matter* **14**, 4901 (2002).
- [26] K. Binder and A. P. Young, *Spin Glasses: Experimental Facts, Theoretical Concepts, and Open Questions*, *Rev. Mod. Phys.* **58**, 801 (1986).
- [27] P. E. Jönsson, R. Mathieu, P. Nordblad, H. Yoshino, H. A. Katori, and A. Ito, *Nonequilibrium Dynamics of Spin Glasses: Examination of the Ghost Domain Scenario*, *Phys. Rev. B* **70**, 174402 (2004).
- [28] L. Lundgren, P. Svedlindh, P. Nordblad, and O. Beckman, *Dynamics of the Relaxation-Time Spectrum in a  $\text{CuMn Spin-Glass}$* , *Phys. Rev. Lett.* **51**, 911 (1983).
- [29] A. K. Kundu, P. Nordblad, and C. N. R. Rao, *Glassy Behaviour of the Ferromagnetic and the Non-Magnetic Insulating States of the Rare Earth Manganates  $\text{Ln}_{0.7}\text{Ba}_{0.3}\text{MnO}_3$  ( $\text{Ln} = \text{Nd}$ ) or  $\text{Gd}$ )*, *J. Phys. Condens. Matter* **18**, 4809 (2006).
- [30] R. Mathieu, P. E. Jönsson, P. Nordblad, H. A. Katori, and A. Ito, *Memory and Chaos in an Ising Spin Glass*, *Phys. Rev. B* **65**, 012411 (2001).
- [31] R. Mathieu, M. Hudl, and P. Nordblad, *Memory and Rejuvenation in a Spin Glass*, *Europhys. Lett.* **90**, 67003 (2010).
- [32] K. Jonason and P. Nordblad, *Sensitivity to Temperature Perturbations of the Aging States in a Re-entrant Ferromagnet*, *Eur. Phys. J. B* **10**, 23 (1999).
- [33] G. V. Pai, S. R. Hassan, H. R. Krishnamurthy, and T. V. Ramakrishnan, *Zero-Temperature Insulator-Metal Transition in Doped Manganites*, *Europhys. Lett.* **64**, 696 (2003).
- [34] T. V. Ramakrishnan, H. R. Krishnamurthy, S. R. Hassan, and G. V. Pai, *Theory of Insulator Metal Transition and Colossal Magnetoresistance in Doped Manganites*, *Phys. Rev. Lett.* **92**, 157203 (2004).
- [35] C. H. Booth, F. Bridges, G. H. Kwei, J. M. Lawrence, A. L. Cornelius, and J. J. Neumeier, *Direct Relationship between Magnetism and  $\text{MnO}_6$  Distortions in  $\text{La}_{1-x}\text{Ca}_x\text{MnO}_3$* , *Phys. Rev. Lett.* **80**, 853 (1998).
- [36] Y. Jiang, F. Bridges, L. Downward, and J. J. Neumeier, *Relationship between Macroscopic Physical Properties and Local Distortions of Low-Doping  $\text{La}_{1-x}\text{Ca}_x\text{MnO}_3$ : An EXAFS Study*, *Phys. Rev. B* **76**, 224428 (2007).
- [37] F. Bridges, L. Downward, J. J. Neumeier, and T. A. Tyson, *Detailed Relationship between Local Structure, Polarons, and Magnetization for  $\text{La}_{1-x}\text{Ca}_x\text{MnO}_3$  ( $0.21 \leq x \leq 0.45$ )*, *Phys. Rev. B* **81**, 184401 (2010).
- [38] G. Papavassiliou, M. Fardis, M. Belesi, T. G. Maris, G. Kallias, M. Pissas, D. Niarchos, C. Dimitropoulos, and J. Dolinsek,  *$^{55}\text{Mn}$  NMR Investigation of Electronic Phase Separation in  $\text{La}_{1-x}\text{Ca}_x\text{MnO}_3$  for  $0.2 \leq x \leq 0.5$* , *Phys. Rev. Lett.* **84**, 761 (2000).